INTERNATIONAL CENTER FOR NUMERICAL METHODS IN ENGINEERING

The Energy Input Spectrum: Scaling Laws and Synthetic Compatible Records

J.E. Hurtado
A.H. Barbat

Publication CIMNE Nº-79, December 1995

The Energy input Spectrum: Scaling Laws and Synthetic Compatible Records

J.E. Hurtado
A. H. Barbat

Publication CIMNE Nº-79, December 1995

International Center for Numerical Methods in Engineering
Gran Capitán s/n, 08034 Barcelona, Spain

THE ENERGY INPUT SPECTRUM: SCALING LAWS AND SYNTHETIC COMPATIBLE RECORDS

JORGE E. HURTADO

National University of Colombia, Apartado 127, Manizales, Colombia

ALEX H. BARBAT

Technical University of Catalonia, c/ Gran Capitán, s/n, Barcelona 08034, Spain

SUMMARY

A method for predicting the seismic energy input spectrum is presented. The method is based on the analytical relationships linking this spectrum and other measures of earthquake energy such as power spectrum and Arias intensity, and the results of the statistical analysis made on 120 strong motion records. Upon the same relationships, a method for simulating artificial accelerograms compatible with a prescribed energy input spectrum is also developed. This procedure is used for the calculation of damage indexes for reinforced concrete single-degree-of freedom-systems, corresponding to types of energy input spectra and different ground motion durations.

INTRODUCTION

Both theoretical and experimental research conducted in the last years have shown that the low cycle fatigue resulting from the repetition of inelastic cycles has a very important role in the structural seismic damage. Due to the difficulties in predicting the amplitude and sequence of those cycles, the fatigue damage effects are usually associated in a simplified manner with earthquake duration and/or energy input. Upon the so-called energy input spectrum, Akiyama[1] developed in the eighties a design method for buildings. At the same time, the dissipated energy was incorporated by Park and Ang [2] in the calculation of a damage index for reinforced concrete elements and these results were then combined by Park *et al.*[3] with the results obtained by Akiyama for the computation of an energy-weighted damage index of a whole reinforced concrete building. In the last years, important contributions to the understanding and use of the energy concepts and low cycle fatigue in earthquake resistant analysis and design have been presented by Uang and Bertero[4], Fajfar and Vidic[5], Cosenza *et al.*[6], among others.[7-13]

One of the difficuties in using the energy concepts in design is, however, that methods for predicting the energy input spectrum are scarce and not generally applicable. As it will be shown later, the proposal of a two-line smoothed spectrum made by Akiyama[1,18] corresponds only to certain cases of energy bandwidth. Recently Fajfar and Vidic[5] proposed a method that is based on the

well-known Newmark-Hall response spectrum and statistical analysis for the assessment of the energy input corresponding to two classes of nonlinear models, and Kuwamura *et al.* [14] developed a procedure that requires the knowledge of Fourier amplitude spectrum for predicting the elastic energy input.

In this paper, a procedure for estimating the energy input spectrum, that uses the statistical results of the analysis of 120 strong motion records and takes into account some analytical relationships of this spectrum with other energy characteristics of the earthquake events is presented. As the emphasis of the study is made on the frequency content and maximum values of the spectrum, the analysis was performed for elastic single-degree-of-freedom systems with 10 percent of damping ratio, whose energy input spectrum is an envelope of the spectra of nonlinear systems usually found in practice[1]. As a result, a simple method for drawing smoothed energy input spectra on the basis of current seismic information is proposed. The main feature of the method is the small number of data and the simplicity required to do such an estimation.

The analytical relationships mentioned above are then used to formulate a method for generating artificial accelerograms compatible with a prescribed energy input spectrum. The comparison of both response and energy input spectra of the simulated records with those of the real ones shows excellent agreement. As an application of the algorithm, a series of accelerograms compatible with the proposed average smooth spectra has been generated to analyse the response of nonlinear systems, using a model that takes into account both strength and stiffness degradation, in order to examine the damage index spectrum of reinforced concrete single degree of freedom systems with respect to different types of energy input spectra and various ground motion durations.

FUNDAMENTAL CONSIDERATIONS

It is well known that the energy input and its distribution in a single degree of freedom structure up to time t of the vibration is given by

$$\int_0^t m\ddot{x}\dot{x}\,\mathrm{d}t + \int_0^t c\dot{x}^2\,\mathrm{d}t + \int_0^t f(x)\dot{x}\,\mathrm{d}t = -\int_0^t m\ddot{x}_g\dot{x}\,\mathrm{d}t \qquad (1)$$

where m is the mass of the structure, c the damping coefficient, $f(x)$ the restoring force, x_g the ground displacement, x the relative displacement of the structure and the dots superimposed indicate time derivatives. This equation corresponds to the formulation that is denoted 'relative' by Uang and Bertero [4,8]. In the 'absolute' formulation the energy input is given in terms of the total motion of the structure with respect to the global axis.

Integrating up to the end of the vibration ($t = t_0$) and splitting the restoring force term into strain and hysteretic energies, the following distribution of the energy input is obtained

$$\frac{m\,\dot{x}^2(t_0)}{2} + W_d + (W_e + W_p) = E \qquad (2)$$

where W_d is the damping energy, W_e the strain energy, W_p the hysteretic energy and E the energy input.

It is obvious that a measure of structural damage can be the ratio of the hysteretic to the input energy. In reference (1), this ratio is calculated using only the viscous damping ratio and estimations of the strain energy, while in reference (5) formulae are proposed for a more refined estimation for two types of nonlinear models.

To avoid mass-dependence of the energy input spectrum, this is usually calculated in a normalized form, by means of an equivalent velocity defined by

$$V_e = \sqrt{\frac{2E}{m}} \tag{3}$$

As it is demonstrated in reference (4), the equivalent velocity tends to the peak ground velocity v as the period tends to infinity. The relative formulation has been preferred in this work because it has clear relationships with the earthquake energy measures used in seismology. As a matter of fact, for a linear system with viscous damping ratio ν, the following integral equation holds: [15]

$$\int_0^\infty \frac{E}{m} d\omega = \frac{\cos^{-1}\nu}{\sqrt{1-\nu^2}} \int_0^t \ddot{x}_g^{\,2} dt \tag{4}$$

where the second integral is proportional to the well-known Arias intensity, I_A with a proportionality factor of $\pi/2g$. In this context this factor will be dropped and the intensity I_A will be calculated as the integral of the squared acceleration.

The last equation implies that the integral of the squared V_e spectrum is related to the intensity I_A by the equation

$$\int_0^\infty V_e^{\,2}(\omega) d\omega = \theta \int_0^t \ddot{x}_g^{\,2} dt \tag{5a}$$

with

$$\theta = \frac{2\cos^{-1}\nu}{\sqrt{1-\nu^2}} \tag{5b}$$

and to the power spectrum, invoking Parseval's theorem, by

$$\int_0^\infty V_e^{\,2}(\omega) d\omega = \frac{\theta}{\pi} \int_0^\infty |X_g(\omega)|^2 d\omega \tag{6}$$

where $|X_g(\omega)|$ is the Fourier amplitude spectrum. For the particular case of null damping, it has been shown in reference (14) that the energy input and Fourier amplitude spectra coincide.

SCALING THE ENERGY INPUT SPECTRUM

The above equations and remarks resume the relationships existing between the energy of the event itself and the energy that is induced in the single-degree-of-freedom linear structure. A particular hypothesis about the V_e spectrum can be drawn from the foregoing statements, namely, that all factors influencing the power spectrum must affect in the same way the energy input spectrum. Among the many existent studies on the power spectrum, attention of the authors was called by a recent work by Sawada *et al.*,[16] in which very close correlations were found between the main characteristics of the power spectrum and the ratio of the maximum acceleration a to maximum velocity v of the ground motion. Specifically, the following findings from that study have been taken into account in this paper:

1. The higher the a/v ratio, the lower the central frequency of the power spectrum. The correlation coefficient between these values taken from Japanese records was 0.88.

2. The lower the a/v ratio, the higher the dispersion of the spectrum about the central frequency. The dispersion was measured using the spectral parameter

$$\delta = \sqrt{1 - \frac{\lambda_2^2}{\lambda_0 \lambda_1}} \tag{7}$$

where λ_i, $i = 0, 1, 2$, is the i-th spectral moment of the power spectrum. In this case, the correlation coefficient was 0.87.

Also, an important influence of the a/v ratio on the amplitude of the acceleration response spectrum has been observed by Zhu *et al.* [17]. In their work the following classification of the a/v ratio is given:

1. Group I: High a/v, for values greater than 12 s^{-1}.
2. Group II: Middle or normal a/v, for values between 8 s^{-1} and 12 s^{-1}.
3. Group III: Low a/v, for values less than 8 s^{-1}.

This classification will be employed in the present study.

The ability of the a/v ratio for describing in a rough manner the attenuation of the seismic waves from the source to the recording site is due to the fact that peak acceleration attenuates more rapidly than peak velocity. However, since attenuation, amplification and changes in frequency content of the seimic waves also occur at the local scale due to the soil conditions, it could be said that the soil influence on the energy input spectrum is implicitly taken into account in the a/v ratio. Therefore, with the purpose of calculating an average energy input spectrum, an alternative method to that of establishing different shapes and values for typical soil conditions, as done in reference (18), could be to classify the spectra according to the a/v ratio, provided that it can be assessed. A regression of this ratio as a function of the event magnitude, epicentral distance and predominant period of the soil layers is given in reference (16).

As an example of the above statement, figure 1 shows the energy spectra of the same earthquake (event 45 of the SMART-1 network) recorded in rock and soil sites[19]. The difference in shape and dominant frequencies between these spectra can be roughly associated with the difference of a/v value of both, which are 11.1 s^{-1} and 5.3 s^{-1} respectively. On the other hand, figure 2 shows three

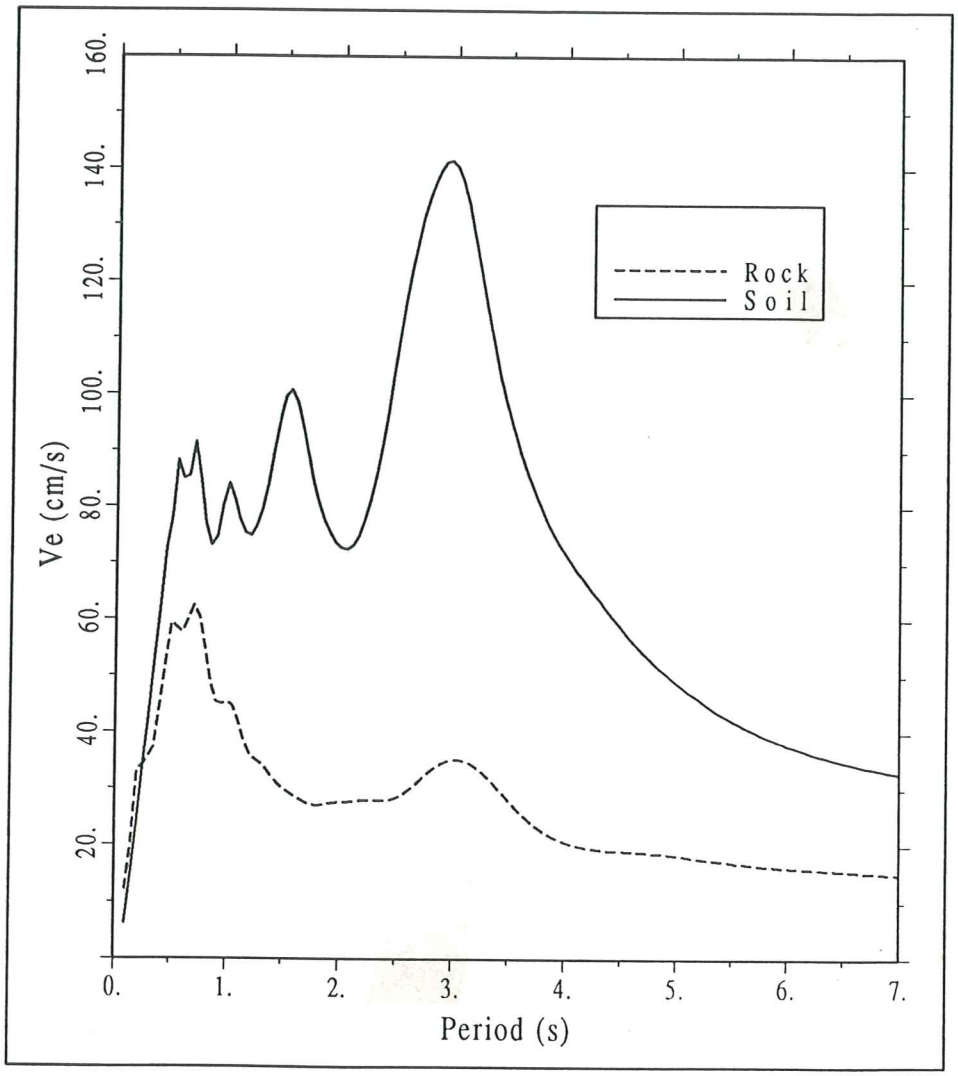

Figure 1. Energy input spectra of the earthquake No. 45 of the SMART-1 network.

energy input spectra, corresponding to the Mexico 1985 earthquake, recorded on very different soil conditions, ranging from rock to soft soil. The lack of significant differences in the shape and predominant periods in this case can be again associated with the similarity of a/v values, which are 2.41, 2.75 and 3.84 s^{-1}.

On the basis of these considerations, the 120 ground motion records corresponding to the horizontal components of the earthquake events listed in the appendix were classified according to the three groups. The energy input spectra were calculated for linear structures having 10 % damping ratio due to the reason stated above. The main results pursued in these numerical analysis were the following:

1. The peak value of normalized V_e spectrum, V_{em}, and its relation with

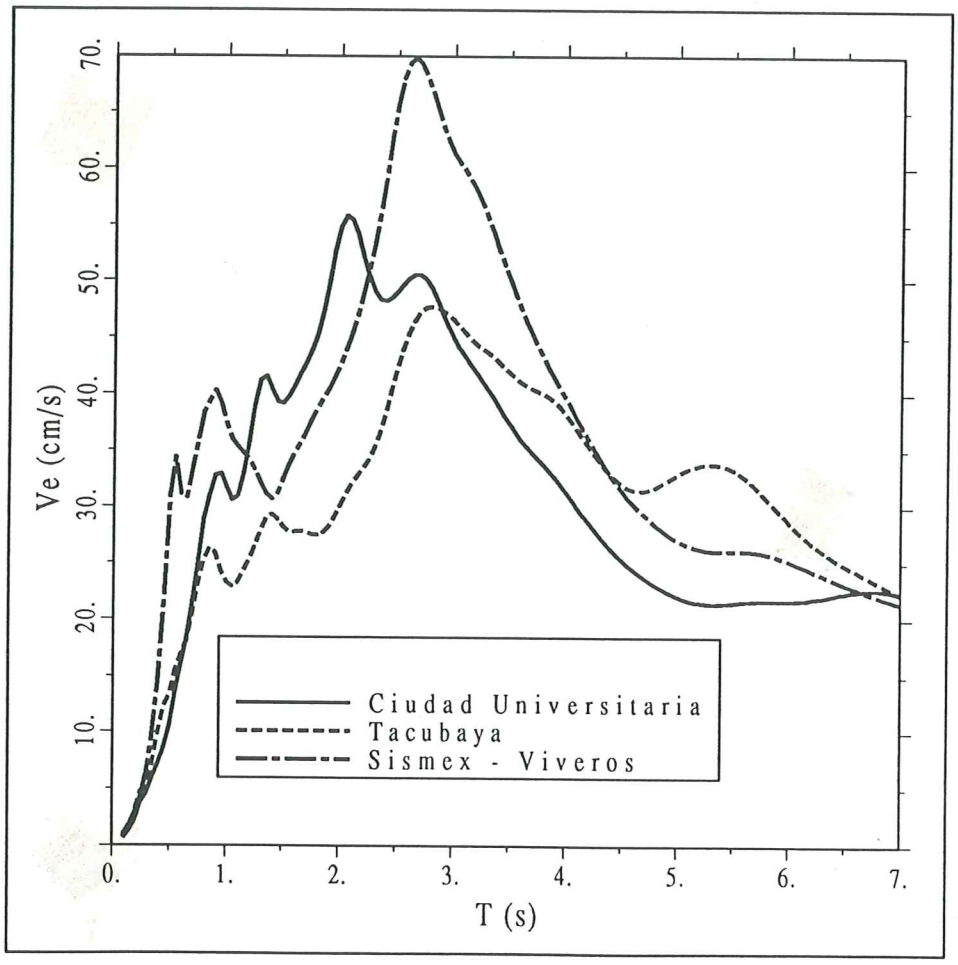

Figure 2. Energy input spectra of the Mexico 1985 earthquake corresponding to three different site conditions: Rock (Ciudad Universitaria), stiff soil (Tacubaya), very soft soil (Sismex-Viveros).

the effective duration of the motion. This value was calculated according to the classical energy-based definition given by Trifunac and Brady[15], as the time elapsed between the instants when the Arias intensity reaches 5 and 95 percent of its total value. The resulting spectra were normalized by the maximum ground acceleration, a, and by the effective root mean square acceleration, calculated as

$$\sigma_{\mathrm{d}}^{\,2} = \frac{\int \ddot{x}_{\mathrm{g}}^{\,2}\,\mathrm{d}t}{t_{\mathrm{d}}} \tag{8}$$

2. The distribution of the energy input on the period range. In this case, due to the sensitivity of the V_{e} spectrum to the duration of the ground motion, each spectrum was normalized by its own maximum value V_{em}, so that the resulting dispersion in the zone of maxima could be attributed only to differences in dominant periods.

The results of the first analysis are shown in figure 3, for the case of nor-

malization with respect to peak acceleration, and in figure 4 for the case of normalization with respect to a value of $\sigma_d = 111.7$ cm/s. In both cases the peak values of the energy spectra were classiffied according to the a/v ratio. It is observed that, while no clear distinction among the peak values appears in the low-duration zone, a higher slope of the relationship of peak values and effective duration of the Group III spectra is evident for long records. The straight lines shown in the figures correspond to the linear regression

$$a_0 + a_1 t_d \tag{9}$$

whose coefficients are given in table 1.

Table 1 Coefficients of the regression analysis of the peak value of the energy input spectrum

Normalization	a/v	a_0	a_1	ρ
$\frac{V_{em}}{a}$	Low	0.251	0.0247	0.792
	Middle	0.309	0.0083	0.391
	High	0.156	0.0131	0.567
$\frac{V_{em}}{\sigma_d}$	Low	0.183	0.0207	0.884
	Middle	0.226	0.0114	0.635
	High	0.109	0.0144	0.717

The correlation coefficients (ρ) for both cases of normalization, given also in the table, indicate that better results can be obtained through the normalization by the root mean square acceleration then those corresponding to normalization by peak ground acceleration, as could be expected on the basis of equation (5a).

Visual examination of the spectral shapes of many of the records showed that in fact the grouping into the three categories was justifiable. The major doubts arose with regard to the group of low a/v values, for which energy input spectra showed the expected wide band nature for the case of effective durations greater than 10s approximately, but a narrower shape for very low durations. The statistical analysis was therefore conducted on the records of groups I and II, and in the case of the third group the records having effective durations of less than 10 s were discarded.

The average normalized spectra are presented in figure 5a. Both the dominant periods and bandwidth of the spectra are rather different for the three groups. It is also evident that a constant spectrum after the ascending branch, as proposed by Akiyama,[1,18] can be associated only with the Group III case.

The following three-branch smoothed energy input spectrum, shown in figure 5.b, is proposed:

$$\frac{V_e}{V_{em}} = \frac{T}{T_1}, \quad T \leq T_1$$

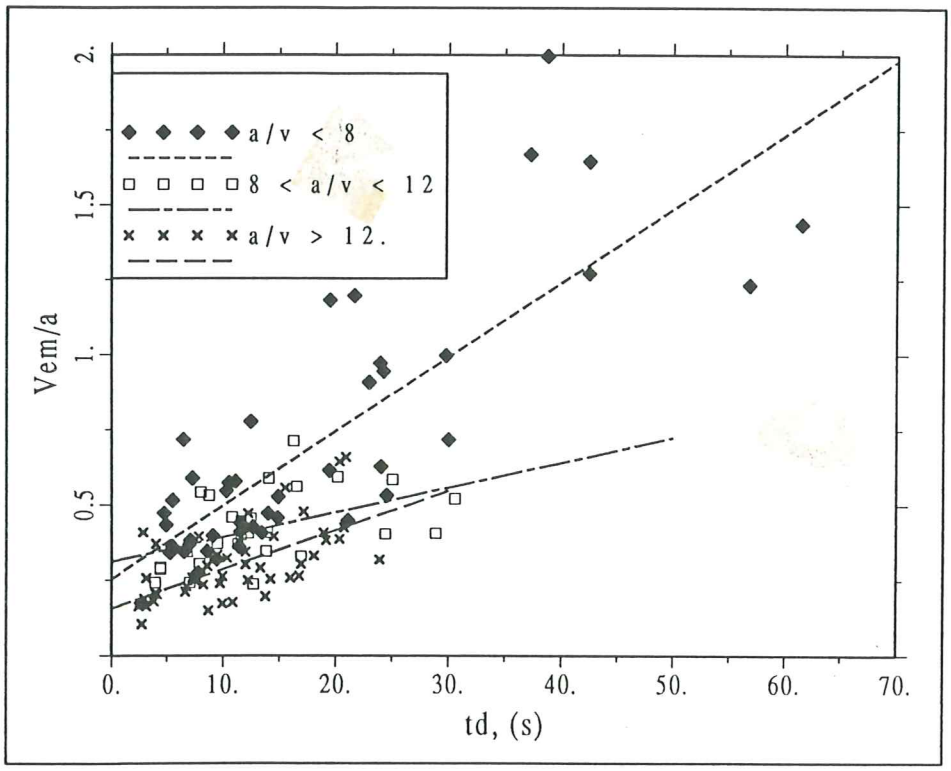

Figure 3. Effective duration vs. peak of energy input spectrum normalized by the peak ground acceleration.

$$\frac{V_e}{V_{em}} = 1, \quad T_1 < T \leq T_2 \tag{10}$$

$$\frac{V_e}{V_{em}} = \left(1 - \frac{v}{V_{em}}\right)\left(\frac{T_2}{T}\right)^d + \frac{v}{V_{em}}, T > T_2$$

where T_1 and T_2 are the periods at the left and right intersections of the horizontal branch, respectively, and d is the decay rate of the right branch.

Recommended values of T_1, T_2 and d, which give a smooth envelope for the calculated average spectra of figure 5.a, are shown in table 2.

The coefficients of variation corresponding to the above analysis are shown in figure 6. In spite of some high values obtained for very low periods, it is clear that the dispersion in the zone of predominant periods is rather low. This suggests that a reliable estimate of an energy input spectrum can be done through the following procedure:

1. Using the seismicity information, estimate the Arias intensity, I_A. An equation for this purpose, characterized by high correlation coefficients, was proposed by Sarma and Yang[20] after the analysis of records of different countries. According to these authors I_A correlates better with the seismicity variables than

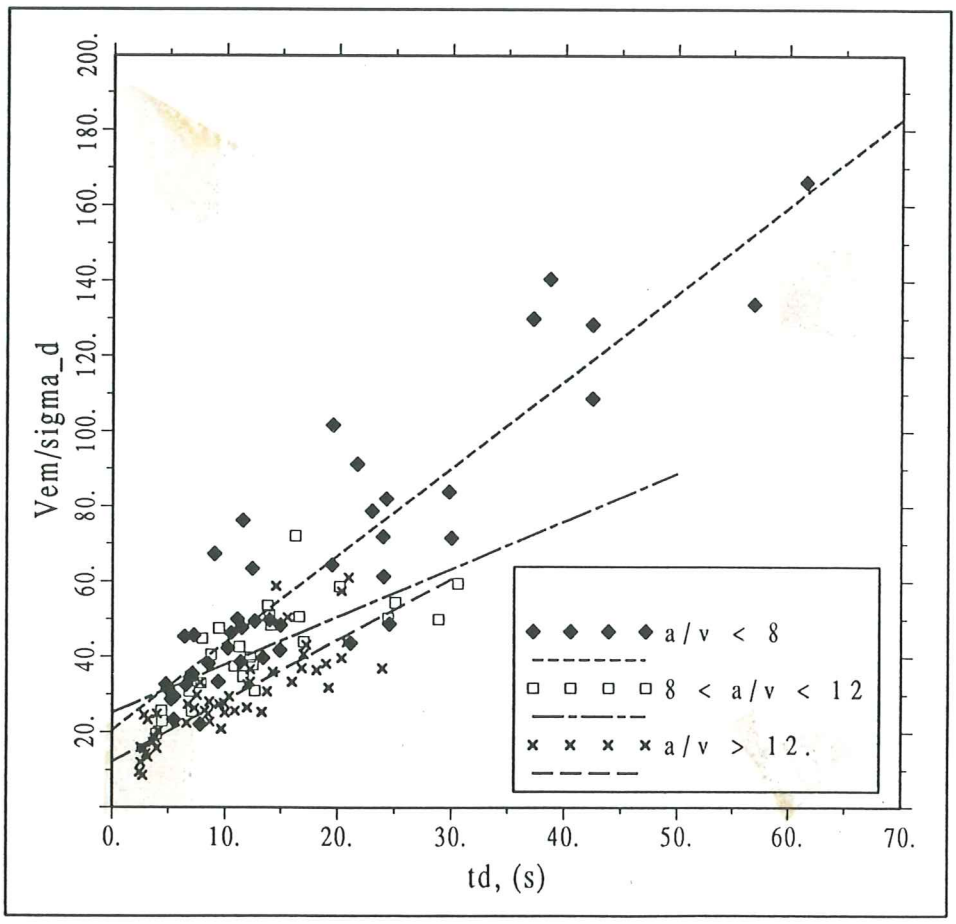

Figure 4. Effective duration vs. peak of energy input spectrum normalized by the effective root mean square acceleration.

the peak acceleration does. For epicentral distances R greater than 30 km the proposed equation is

$$\log I_{\mathrm{A}} = -4.05 + 0.77M - 0.85 \log R - 0.0081R \tag{11}$$

where M is the magnitude of the event. A different equation is given for the case of R less than 30 km.

2. Estimate the effective duration, t_{d}. For U.S. earthquakes, regression equations have been proposed by Trifunac and Brady[15] and Trifunac and Novikova[21].

3. Calculate the peak value and select the spectral shape according to the rules given above. It is prefarable to use the r.m.s. regression equation than the peak acceleration one, as stated before. Also, it is important to note that the area of the squared spectrum must follow the proportionality law given by equation (4), and the asymptotic tendency of V_{e} to v mentioned before. This implies that the following equation holds for the proposed smoothed spectrum

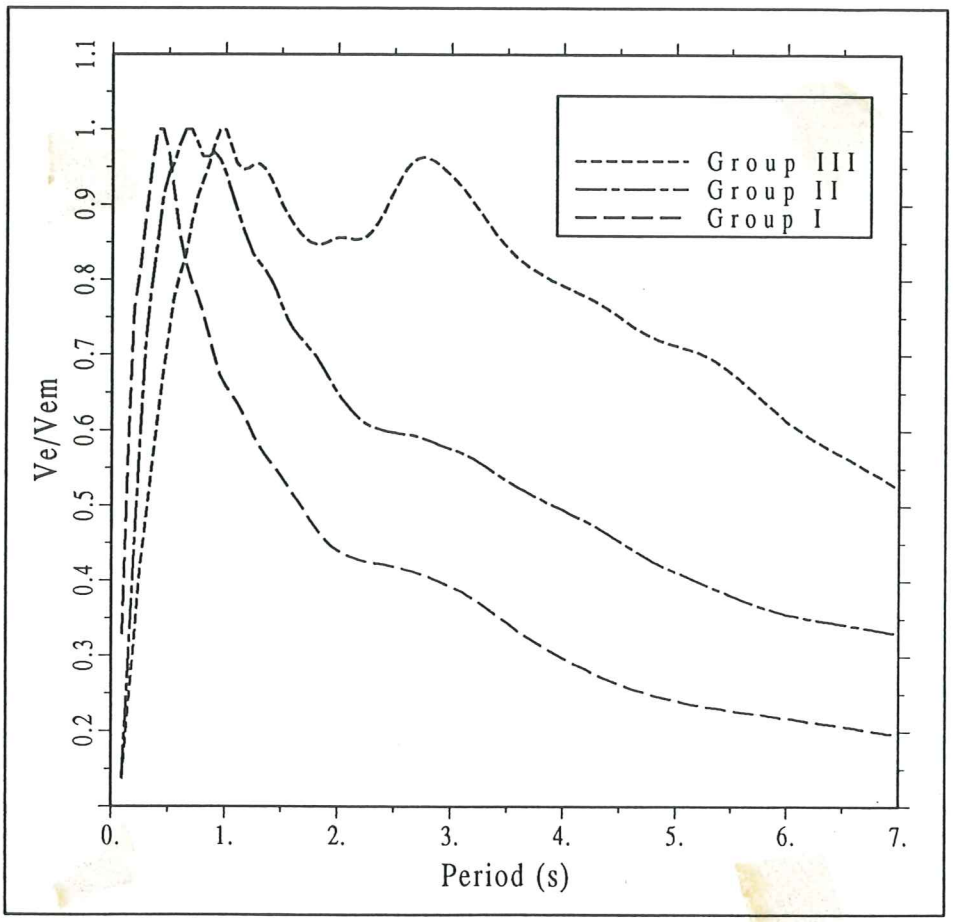

Figure 5a. Average normalized spectra for Groups I, II and III.

Table 2 Parameters of the proposed smoothed spectra

Group	T_1	T_2	d
I	0.3	0.6	0.66
II	0.4	1.0	0.57
III	0.8	2.6	0.53

given in equation (10):

$$(V_{\text{em}} - v)^2 \frac{\omega_2}{1+2d} + 2v(V_{\text{em}} - v)\frac{\omega_2}{1+d} + v^2\omega_2$$

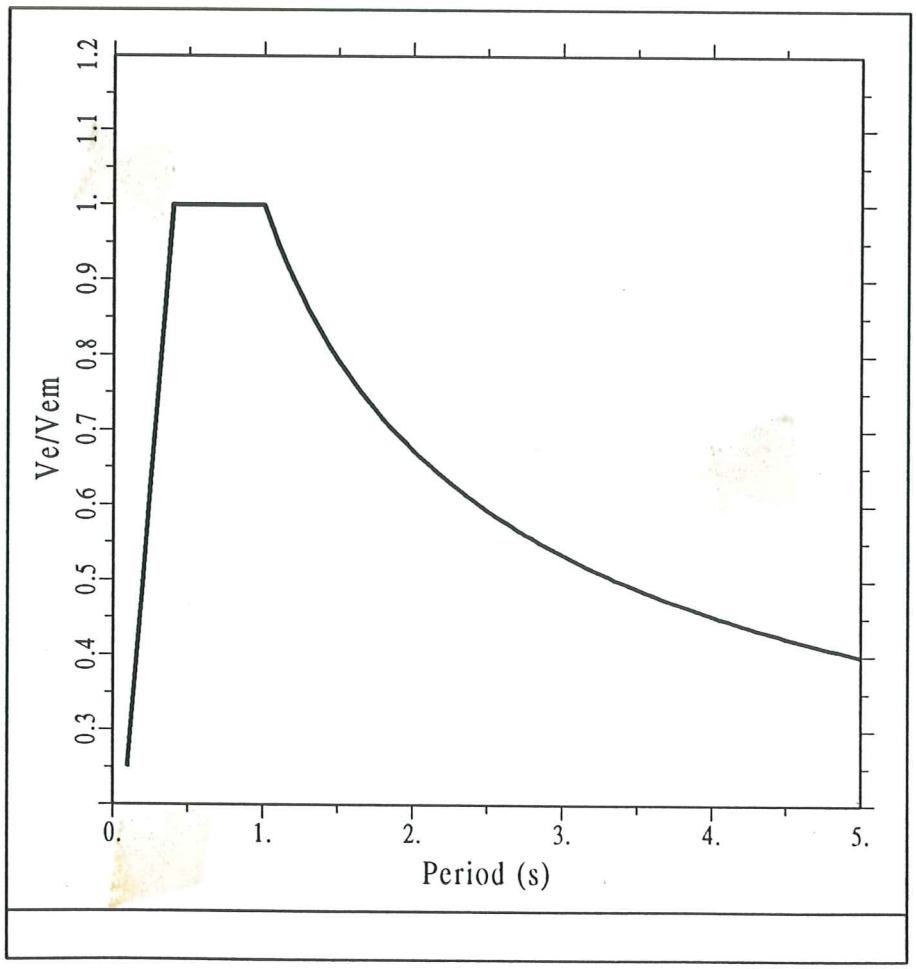

Figure 5b. Proposed smoothed energy input spectrum.

$$+V_{\text{em}}{}^{2}(2\omega_1 - \omega_2) = \theta I_{\text{A}} \tag{12}$$

where ω_1 and ω_2 are the circular frequencies corresponding to T_1 and T_2 respectively. This equation can be used for a final adjustment of the design spectrum.

It is seen that the method proposed for drawing a smoothed energy input spectrum for design purposes is rather simple, since it requires only four ground motion parameters, all of which —the peak ground acceleration and velocity, the Arias intensity and the effective duration— can be estimated using seismicity information. Moreover, the constraints with respect to Arias intensity and peak velocity, e. g. equations (5a) and (12), make it possible to vary or adjust the peak value to a given spectral bandwidth, or vice-versa, without violating the inherent mechanical principles.

SIMULATION OF ACCELEROGRAMS COMPATIBLE WITH A PRESCRIBED ENERGY INPUT SPECTRUM

The power spectral density funtion of an earthquake is usually estimated from a single record by

$$G(\omega) = \frac{|X_g(\omega)|^2}{\pi s_0} \tag{13}$$

where s_0 is the duration of the stationary part of the ground motion. The relationships linking the energy input and power spectra mentioned above suggest that an estimate of $G(\omega)$, could be obtained through

$$G(\omega) = \frac{V_e{}^2(\omega)}{s_0 \theta} \tag{14}$$

Synthetic accelerograms compatible with a prescribed energy input spectrum can then be generated using the function

$$\ddot{x}_g(t) = \xi(t) \Sigma_{i=1}^{n} A(\omega_i) \cos(\omega_i t + \phi_i) \tag{15}$$

where $\xi(t)$ is an envelope function which gives non-stationarity in amplitude to the artificial signal, $A(\omega_i)$ are the amplitudes of a stationary signal, and ϕ_i are random phase angles with a uniform probability density funtion in the range $[0, 2\pi]$. The amplitudes are calculated after dicretization of the power espectral density funcion in several intervals of size $\Delta\omega$

$$A(\omega_i) = \sqrt{2G(\omega_i)\Delta\omega} \tag{16}$$

The value of s_0 could be calculated by an implicit equation proposed by Vanmarcke and Lai[22], as a function of the dominant period in the strong motion phase, the Arias intensity and the peak ground acceleration. However, the use of this equation does not always provide energy spectra close to the given one, due to the dependence of s_0 on the peak ground acceleration, which is a random variable poorly correlated with the peak value of the V_e spectrum, as shown above. In order to obtain better results, an iterative procedure is necessary, which implies sequential scaling of the acceleration values of the record until the allowed tolerance with respect to the given V_e is reached.

Among the several forms that are proposed in the literature for the envelope function, it is the thought of the authors that the one proposed by Tung et al.[23] is adequate for the present purpose, because it is normalized with respect to the effective duration that is to be given to the synthetic record. This envelope is defined by

$$\xi(t) = Z \sin^{\alpha}[\pi(\frac{t}{t_d})^{\beta}] \tag{17}$$

where Z is given by

$$Z = \sqrt{\frac{10/9}{\int_0^1 \sin^{2\alpha}(\pi\tau^{\beta})d\tau}}\sigma_d \tag{18}$$

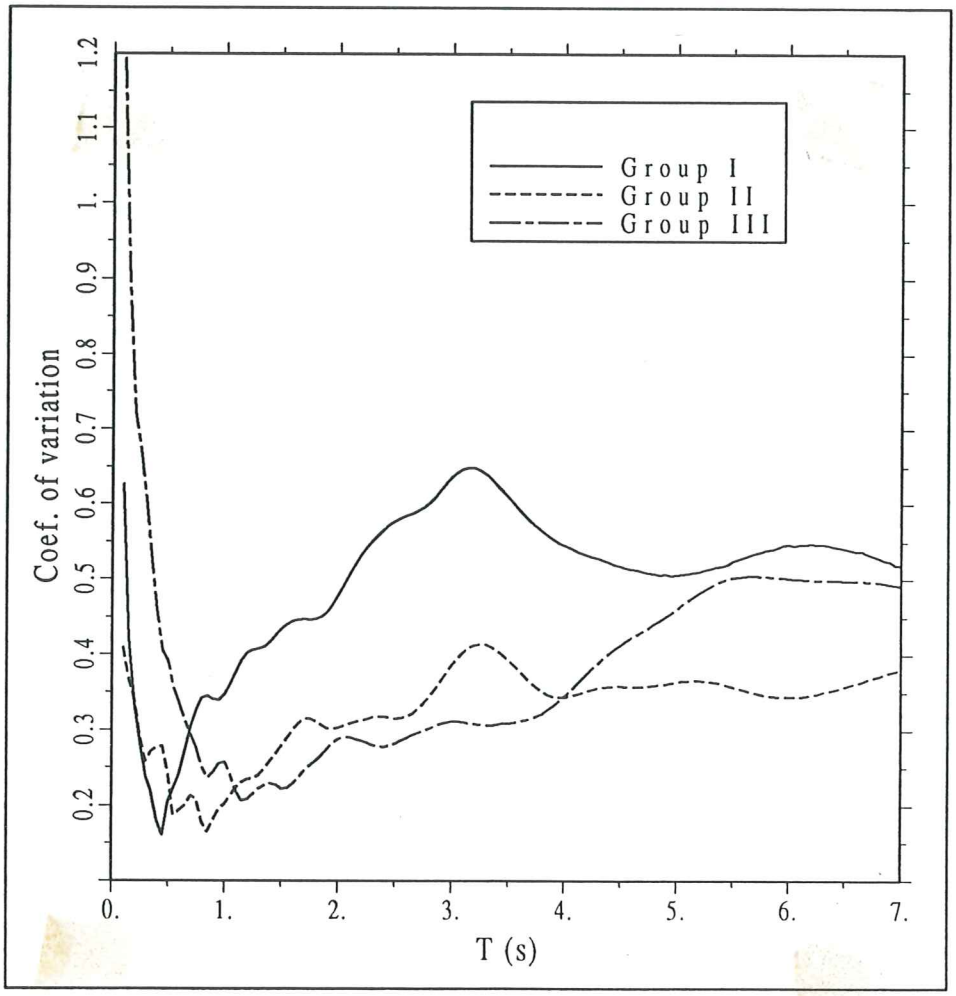

Figure 6. Coefficients of variation of the average normalized energy input spectra.

and the parameters α and β have been statistically related to t_d for soil and rock site conditions. The value of σ_d can be calculated directy from the target spectrum as

$$\sigma_d^{\,2} = \frac{1}{t_d \theta} \int_0^{\infty} V_e^{\,2} \, d\omega \tag{19}$$

Figures 7a and 7b show the Hachinoe earthquake record and one artificial accelerogram generated by this method. The differences between them arise from the need of giving the same energy of the original record to the synthetic one in a rather shorter duration. But, as figure 8a shows, the agreement between the corresponding energy spectra is very good. Moreover, it is important to observe that this is also the case with the acceleration response spectra of both real and simulated records, as it is shown in figure 8b.

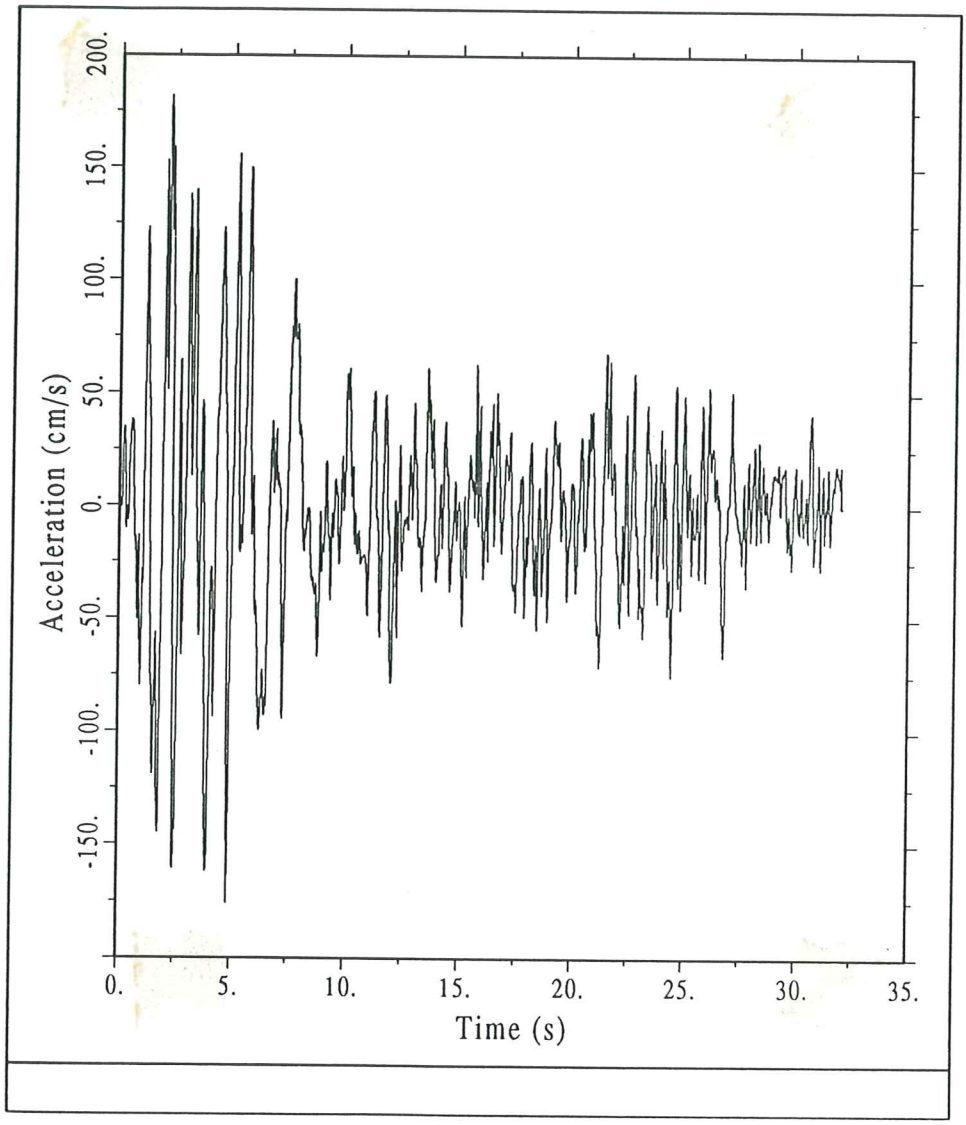

Figure 7a. Record of Tokachi-oki earthquake in Hachinoe harbor, E-W component.

EFFECTS ON DAMAGE OF SPECTRUM TYPE AND DURATION

The proposed algorithm can be used for different purposes of seismic analysis, such us nonlinear design of structures, fatigue analysis, etc. In the present paper, it has been utilized to generate many synthetic accelerograms compatible with the smoothed energy input spectra presented in this paper, with the aim of having an overview on the effect of shape of energy spectrum and ground motion duration on the damage of single-degree-of-freedom reinforced concrete structures. The damage index proposed by Park and Ang[2]

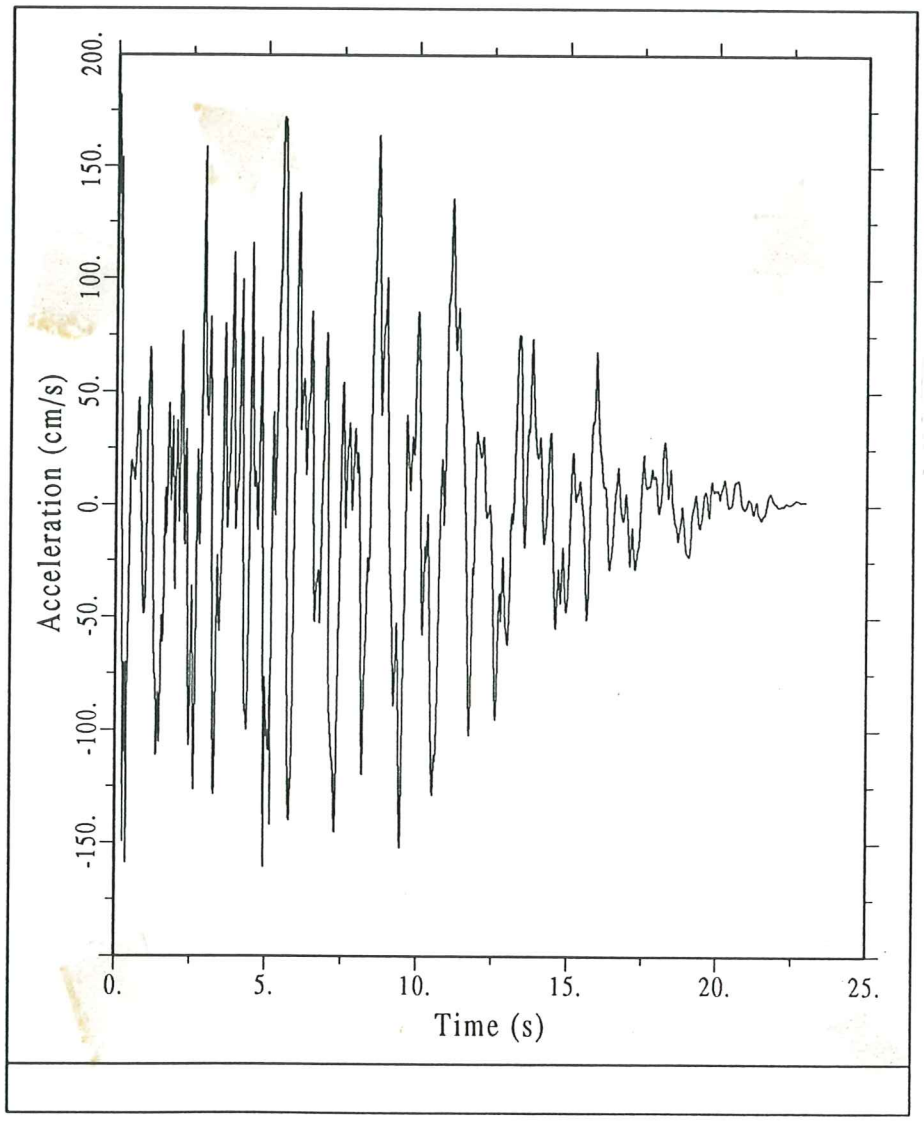

Figure 7b. Synthetic record generated from the energy input spectrum of Hachinoe record.

$$D = \frac{1}{\mu_u}(\mu + \beta \frac{W_{\mathrm{p}}}{F_{\mathrm{y}} d_{\mathrm{y}}}) \tag{20}$$

has been used. In this equation μ_u is the maximum capacity of monotonic ductility, F_{y} and d_{y} are the strength and yield displacement, respectively, and β is an empirical parameter that is associated with the degradation of structural properties with the increasing energy dissipation. For the calculation of the maximum ductility demand, μ, and hysteretic energy W_{p}, use was made in the present case of the endochronic model proposed by Bouc[24] and developed by Baber and Wen[25], which has found wide application in random vibration[26] as well as in the development of deterministic earthquake algorithms of analysis.[27]

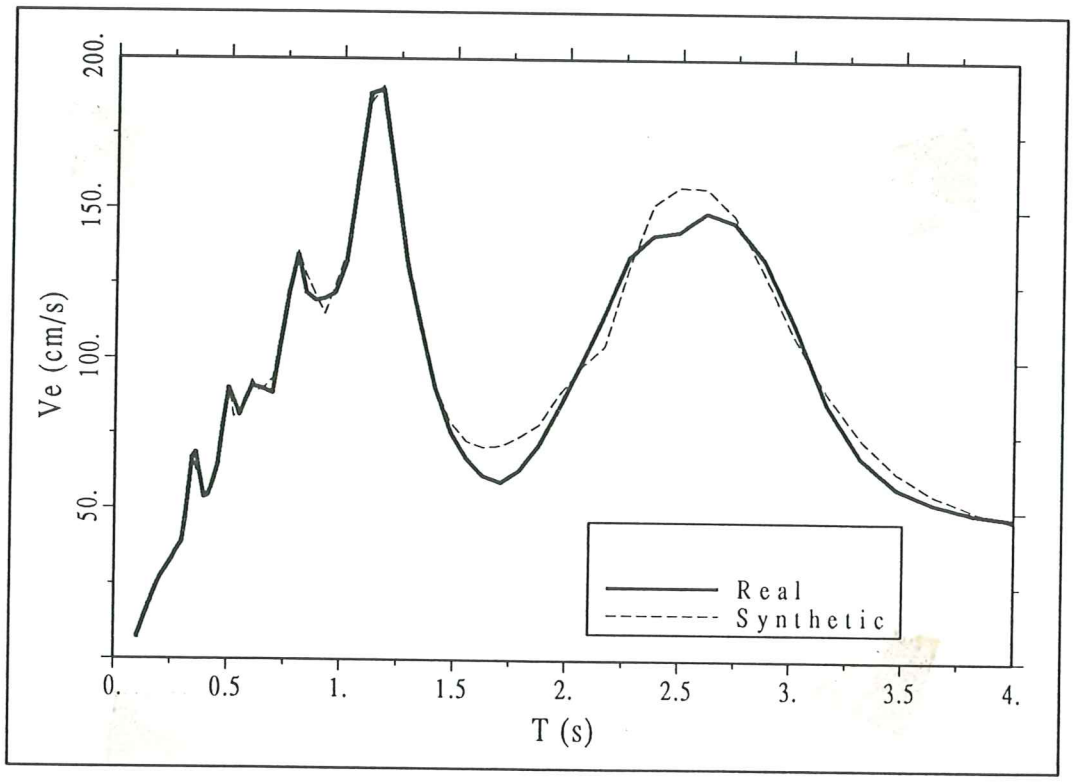

Figure 8a. Energy input spectra of Hachinoe and synthetic records.

In this model the restoring force is given by the sum of a linear component and a nonlinear one

$$f(x) = \alpha kx + (1 - \alpha)kz \tag{21}$$

where z is a non-linear function with displacement units, given by

$$\dot{z} = [A\dot{x} - \nu(\epsilon|\dot{x}||z|^{n-1}z + \gamma\dot{x}|z|^n)]/\eta \tag{22}$$

in which A, ν, η, ϵ, n and γ are material-dependent parameters. Degradation of stiffness and strength can be modelled by varying the first three parameters as functions of the dissipated energy. In the present case, the value of the parameters and the degradation scheme used were those determined by Sues *et al.* [28] by structural identification techniques.

The analysis involved the generation of three accelerograms compatible with the smoothed spectra given by equation (10) for groups I and III, having effective durations of 10, 25 and 40 s (making a total number of accelerograms equal to

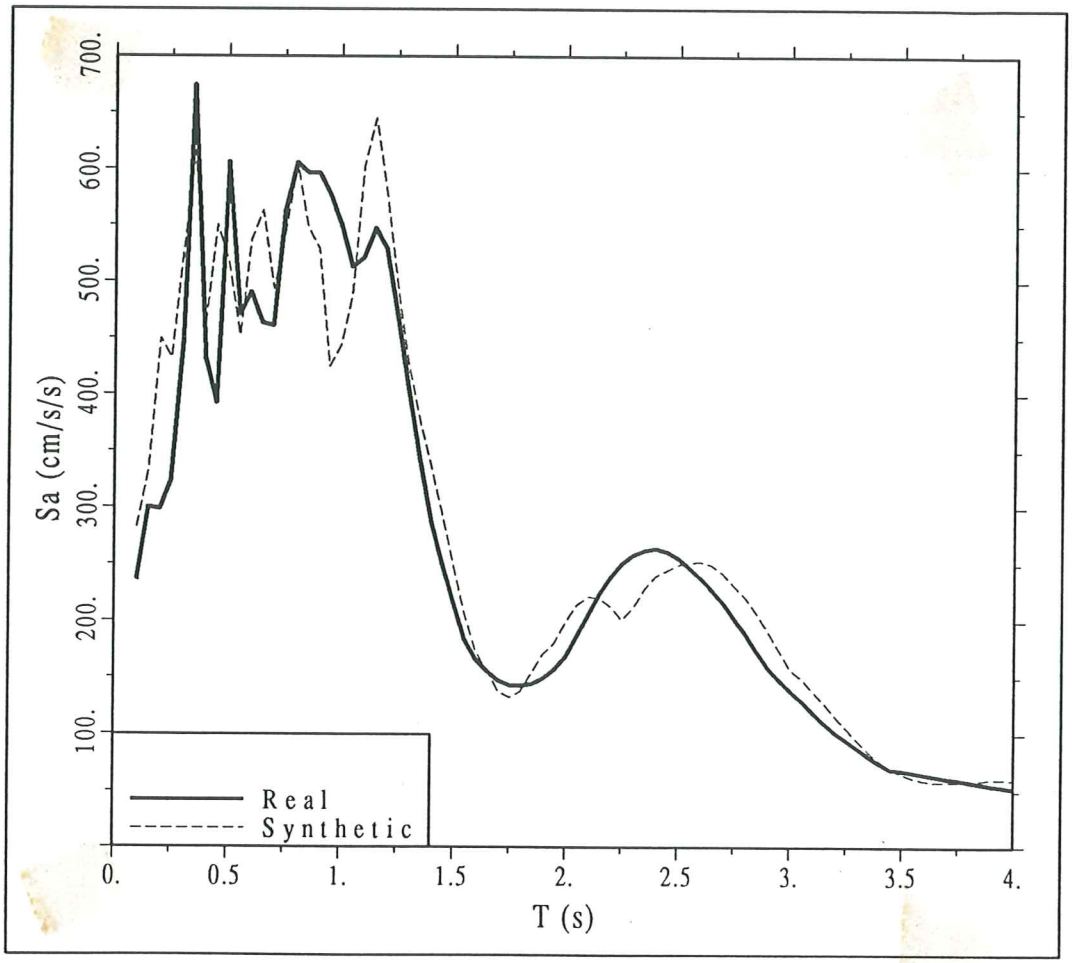

Figure 8b. Acceleration response spectra of Hachinoe and synthetic records.

18), and the results of each case were averaged. The strength of the system was defined in a way that is usual in seismic codes, namely,

$$F_y = \frac{S_a}{R} W \tag{23}$$

where S_a is the elastic response of a system having the same stiffness as the initial one of the nonlinear system, W the weight of the structure and R is a reduction factor, which usually takes values in the range 1.5 to 7. Computations were made for R equal to 2, 4 and 6 in each case and with a value of μ_u equal to 6 used in all cases.

As shown in figure 9, the acceleration response spectra of synthetic records generated by the present method from a smoothed V_e spectrum are also smooth enough so that the results of damage index computation will not be dependent on the peaked shape which is usual in the elastic S_a spectrum of real earthquakes, especially in the low period range. It is for this reason that synthetic rather than real records were preferred for this part of the present study.

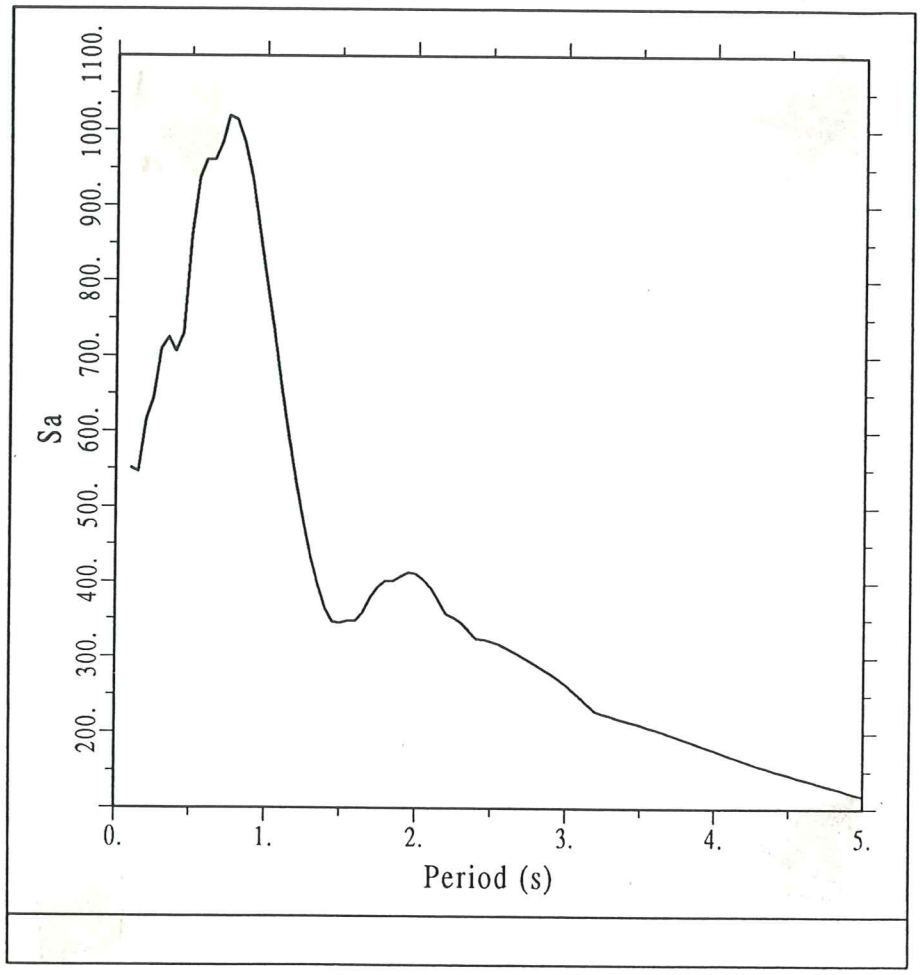

Figure 9. Acceleration spectrum of a synthetic record compatible with a smoothed energy input spectrum.

In order to examine the effect of strength and stiffness degradation, some analyses were performed using the same model parameters with and without considering their degradation. Figures 10 and 11 show the D spectra of those cases using accelerograms of 10s of effective duration compatible with Group I and Group III spectra, respectively. It is observed in these figures that there is a greater sensitivity to degradation in the last case than in the former one for all values of R. In the Group I case, the D spectrum is more or less the same with or without degradation for $R = 4$, and even a surprising result was obtained in the case of $R = 2$, where the damage index of non-degrading structures was higher than those of degrading ones. Conversely, in the case of low a/v values, the D values of degrading models are systematically higher than those corresponding to non-degrading systems.

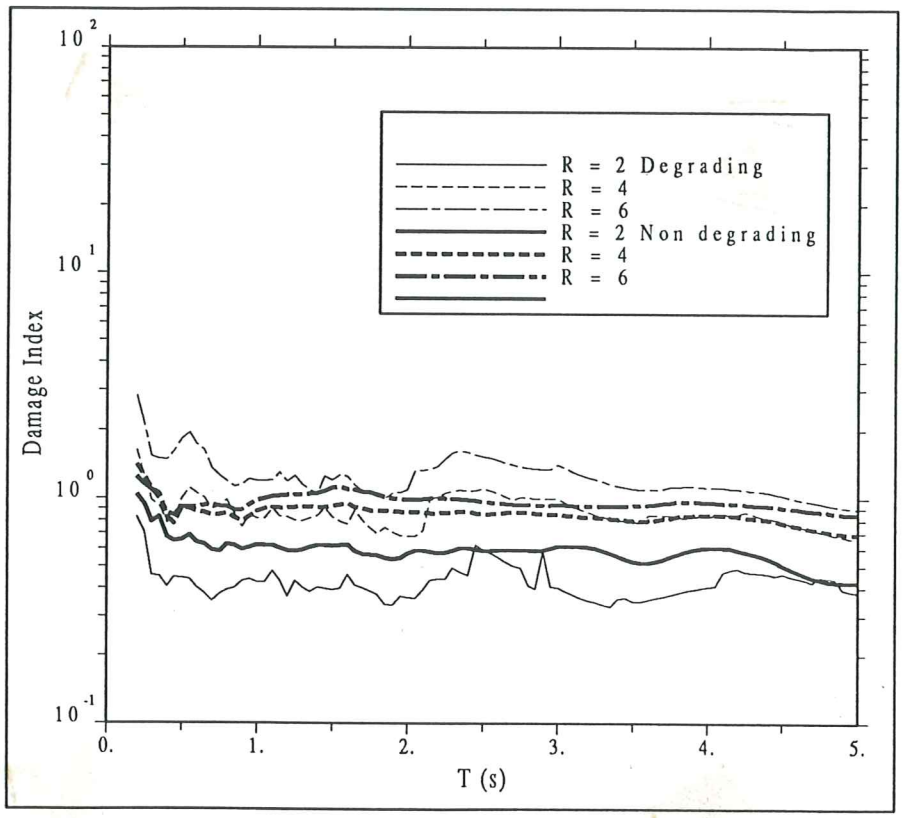

Figure 10. Damage index spectra. Effect of degradation using Group I compatible records.

This difference in sensitivity with respect to the bandwidth of energy input can be explained by the fact that Group I spectrum exhibits high energy values only in a very narrow band, located in the zone of low periods, while in Group III case high energy values are located in a wider zone of lower frequencies. As a consequence, in the last case, high energies are found in the range of periods similar to the instantaneous periods of the degraded structure, with the result of further degradation and so on until the end of the ground motion.

The different values taken by the D spectrum in both cases can be seen in the direct comparison for degrading models shown in figure 12, corresponding to accelerograms of 40s of effective duration and models with $R = 2$ and $R = 6$. It is clear that the marked difference between these extreme cases of type of energy bandwidth affects mainly structures with periods up to 1.5 s, after which the D values are similar.

It is assumed that an intermediate behavior should be observed in the case of Group II, but no attempts were made in the present study to demonstrate this statement.

The effect of ground motion duration is shown in figure 13, for Group III compatible accelerograms and degrading models of $R = 2$ and $R = 6$. A marked

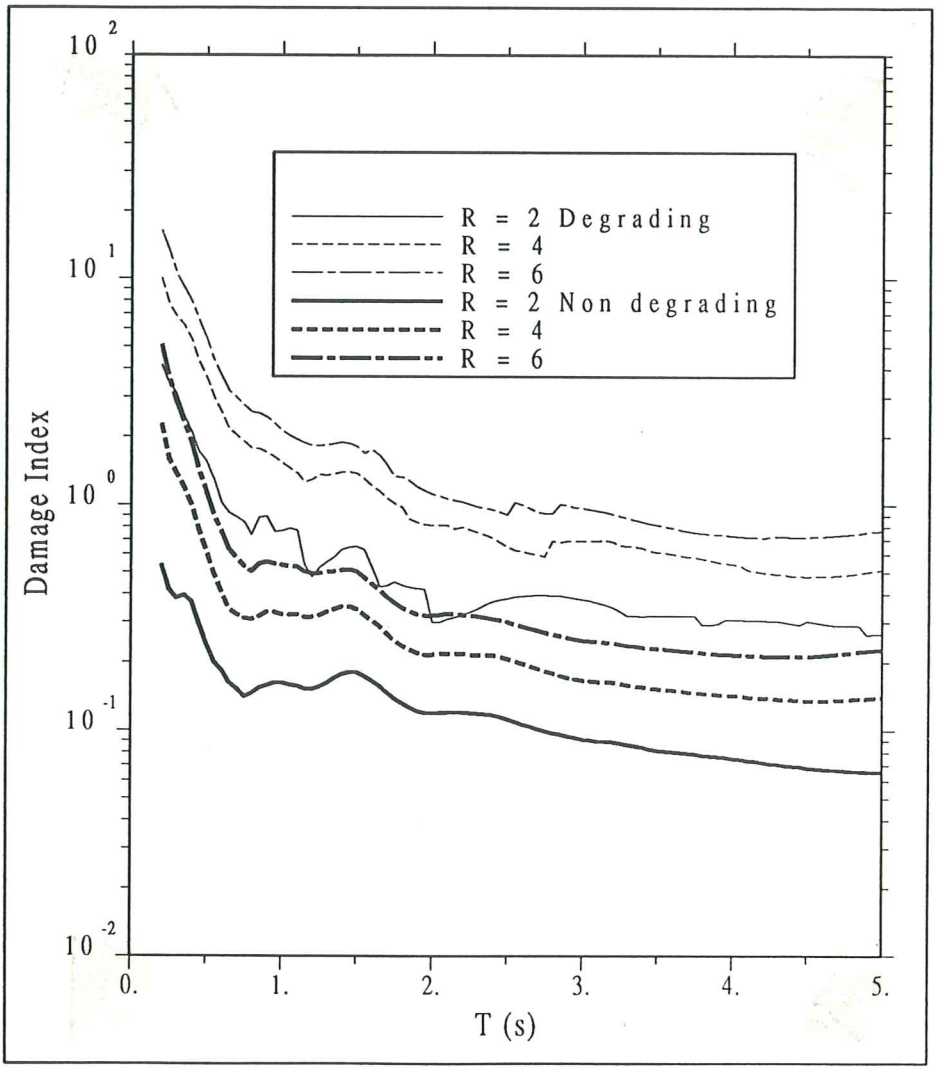

Figure 11. Damage index spectra. Effect of degradation using Group III compatible records.

influence of duration is clearly observed up to periods of about 1.5s, after which the positive damaging effect of duration seems not to be as obvious as expected, given that D values in this zone are roughly the same for all ground motion durations.

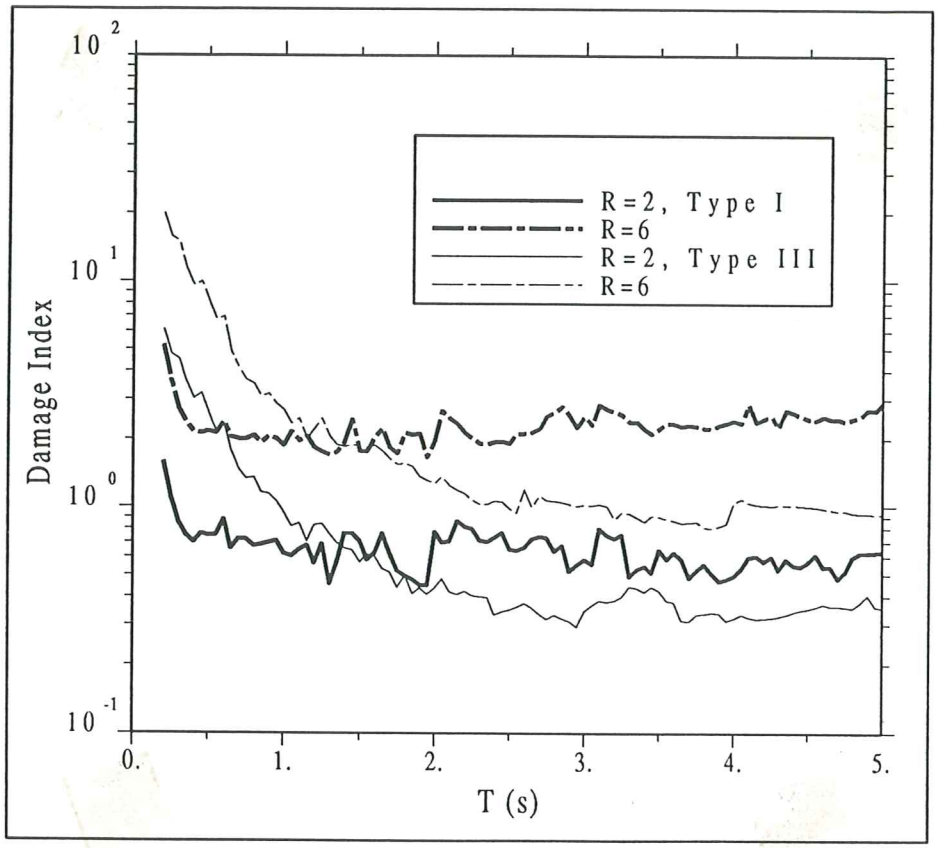

Figure 12. Effect of type of energy input spectrum on damage index.

CONCLUSIONS

The following conclusions can be drawn from the present research:

1. The analitycal relationships existing between the energy input and power spectra and the close correlations of the main parameters of the latter with the a/v ratio allow the classification of V_e spectra into three groups, corresponding to high, middle and low a/v ratio.

2. Average shapes of the energy input spectra for elastic structures with 10 percent damping, normalized with respect to the peak value, and regression equations for estimating the latter, were obtained after the analysis of 120 strong motion records. The statistics of the parameters involved shows that the drawing of a smoothed energy input spectrum upon this basis is reliable. Thus, a procedure to perform such an estimation is presented, which makes use of the constraints imposed on the V_e spectrum by the Arias intensity and peak velocity.

3. A procedure for generating synthetic accelerograms compatible with a prescribed energy spectrum was presented. The procedure was used in this study for simulating the effects of the spectrum shape and ground motion duration

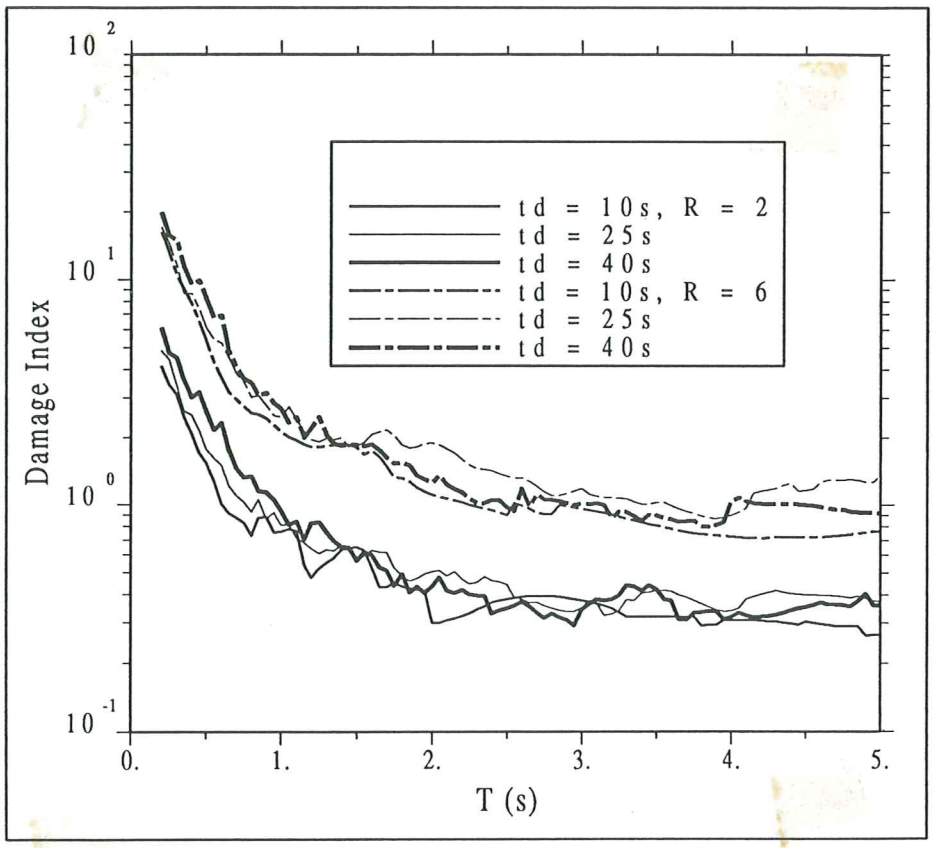

Figure 13. Effect of ground motion duration on damage index using Group III records.

on the structural damage of simple degrading systems of Bouc-Wen-Baber type. The main conclusions drawn from this simulation study are that (1), degradation is more severe in the case of records for Group III, characterized with low a/v ratio and wide spectral bandwidth, than those of Group I, having high a/v and extremely narrow band nature; (2), the positive effect of ground motion duration on damage is conspicuous up to a period of about 1.5 s., being not so clear for higher periods.

ACKNOWLEDGMENTS

Financial supports for doing the present research at the Technical University of Catalonia, consisting of a scholarship given to the first author, was received from the Colombian Institute for the Development of Science and Technology, COLCIENCIAS and the National University of Colombia. These supports are gratefully acknowledged.

References

1. H. Akiyama, *Earthquake-resistant limit-state design of buildings*, University of Tokio Press, Tokio, 1985.
2. Y. J. Park and A. H. S. Ang, "Mechanistic seismic damage model for reinforced concrete", *Journal of Engineering Mechanics, ASCE*, **111 (4)**, 722-739 (1985)
3. Y. J. Park, A. H. S. Ang and Y. K. Wen, "Seismic damage assessment of reinforced concrete buildings", *Journal of Engineering Mechanics, ASCE*, **111 (4)**, 740-757 (1985)
4. C. M. Uang and V. Bertero, "Evaluation of seismic energy in structures" *Earthquake Engineering and Structural Dynamics*, **18**, 77-90 (1990)
5. P. Fajfar and T. Vidic, "Consistent inelastic design spectra: hysteretic and input energy" *Earthquake Engineering and Structural Dynamics*, **23**, 523-537 (1994)
6. E. Cosenza, G. Manfredi and R. Ramasco, "The use of damage functionals in earthquake engineering: a comparison between different methods", *Earthquake Engineering and Structural Dynamics*, **22**, 855-868 (1993)
7. T. Minami and Y. Osawa, "Elastic-plastic response spectra for different hysteretic rules" *Earthquake Engineering and Structural Dynamics*, **16**, 555-568 (1988)
8. C. M. Uang and V. Bertero, "Use of energy as a design criterion in earthquake resistant design" Earthquake Engineering Research Center, *Report No. EERC 88-18* (1988)
9. H. Banon and D. Veneziano, "Seismic Safety of Reinforced Concrete Members and Structures", *Earthquake Engineering and Structural Dynamics*, **10**, 179-193 (1982)
10. T. F. Zahrah and W. J. Hall, "Earthquake energy absortion in SDOF structures", *Journal of Structural Engineering, ASCE*, **110(8)**, 1757-1771 (1984)
11. G. D. Jeong and W. Iwan, "The effect of earthquake duration on the damage of structures" *Earthquake Engineering and Structural Dynamics*, **16**, 1201-1211 (1988)
12. G. H. Powell and R. Allahabadi, "Seismic damage prediction by deterministic methods: concepts and procedures" *Earthquake Engineering and Structural Dynamics*, **16**, 719-734 (1988)
13. T. Vidic, P. Fajfar and M. Fischinger, "Consistent inelastic design spectra: strenght and displacement" *Earthquake Engineering and Structural Dynamics*, **23**, 507-521 (1994)
14. H. Kuwamura, Y. Kirino and H. Akiyama, "Prediction of earthquake energy input from smoothed Fourier amplitude spectrum" *Earthquake Engineering and Structural Dynamics*, **23**, 1125-1137 (1994)
15. M. D. Trifunac and A. G. Brady, "A study of the duration of strong earthquake ground motions ", *Bulletin of Seismological Society of America*, **65(3)**, 581-626 (1975)
16. T. Sawada, K. Hirao, O. Tsujihara, H. Yamamoto, "Relationship between

maximum amplitude ratio ($\frac{a}{v}$, $\frac{ad}{v^2}$) and spectral parameters of earthquake ground motion", *Proceedings of the 10th World Conference on Earthquake Engineering*, Madrid, **2**, 617-622 (1992)
17. T. J. Zhu, A. C. Heidebrecht and W. K. Tso, "Effect of peak ground acceleration to velocity ratio on ductility demand of inelastic systems", *Earthquake Engineering and Structural Dynamics*, **16**, 63-79 (1988)
18. H.Akiyama, "Design energy spectra for specific ground conditions". *Proceedings of the International Workshop on Recent Developments in Base Isolation Techniques*, Tokio, (1992)
19. A. Roca, "Determination of Seismic Near Field using Accelerometer Networks" Ph. D Thesis, Universidad Complutense, Madrid, (1992) (in Spanish)
20. S. K. Sarma and K. S. Yang, "An evaluation of strong motion records and a new parameter A_{95}" *Earthquake Engineering and Structural Dynamics*, **15**, 119-132 (1987)
21. E. I. Novikova and M. D. Trifunac, "Duration of strong Ground Motion in terms of Earthquake Magnitude, Epicentral Distance, Site conditions and Site Geometry", *Earthquake Engineering and Structural Dynamics*, **23**, 1023-1043 (1994)
22. E. H. Vanmarcke and S. P. Lai, "Strong motion duration and RMS amplitude of earthquake records", *Bulletin of Seismological Society of America*, **70(4)**, 1293-1307 (1980)
23. A. T. Y. Tung, J. N. Wang, A. Kiremidjian and E. Kavazanjian, "Statistical parameters of AM and PSD functions for the generation of site-specific strong ground motions", *Proceedings of the 10th World Conference on Earthquake Engineering*, Madrid, **2**, 867-872 (1992)
24. R. Bouc, "Forced Vibrations of Mechanical Systems with Hysteresis", *Proceedings of the Fourth Conference on Nonlinear Oscillations*, Prague, (1967)
25. T. T. Baber and Y. K. Wen, "Stochastic equivalent linearization for hysteretic, degrading, multistory structures". *Civil Engineering Studies SRS No 471*, Department of Civil Engineering, University of Illinois, Urbana (1980)
26. F. Casciatti, L. Faravelli, *Fragility Analysis of Complex Structural Systems*, Research Studies Press, Taunton, 1991.
27. S. Kunnath, A. Reinhorn, "Inelastic Three-Dimensional Response Analysis of Reinforced Concrete Building Structures (IDARC-3D)". *Technical Report NCEER-89-0011* State University of New York at Buffalo (1989)
28. R. H. Sues, S. T. Mau and Y. K. Wen, "Systems Identification of Degrading Hysteretic Restoring Forces", *Journal of Engineering Mechanics, ASCE*, **114(5)**, 833-841 1988

Appendix

List of records used in the study

Earthquake	Record	Date
Friuli	Forgaria	76.09.15
Friuli	San Rocco	76.09.15
Parkfield	Temblor	66.06.27
Tokachi oki	Hachinoe Harbour (*)	68.05.16
Miyagi ken oki	Tohoku University (*)	78.06.12
Eureka	Eureka Federal Building	54.12.21
Loma Prieta	Capitola Station (*)	89.10.18
Loma Prieta	Santa Cruz Mountains	89.10.18
Loma Prieta	Stanford Parking	89.10.18
Loma Prieta	Gilroy, Gavilan College	89.10.18
Loma Prieta	Halls Valley	89.10.18
Loma Prieta	Monterey City Hall	89.10.18
Loma Prieta	Palo Alto VA Hospital	89.10.18
Loma Prieta	Cliff House	89.10.18
Loma Prieta	Corralitos Eureka Canyon	89.10.18
Loma Prieta	Diamond Heights	89.10.18
Loma Prieta	San Francisco Int. Airport	89.10.18
Loma Prieta	Telegraph Hill	89.10.18
Loma Prieta	Rincon Hill	89.10.18
Loma Prieta	Pacific Heights	89.10.18
Loma Prieta	Presidio	89.10.18
Chile	LLolleo	85.03.03
Chile	Viña del Mar	85.03.03
Chile	Valparaiso	85.03.03
Mexico	Ciudad Universitaria	85.09.19
Mexico	Sismex Viveros	85.09.19
Mexico	Tacubaya	85.09.19
Imperial Valley	El Centro	40.05.18
Ferndale	Ferndale City Hall	51.10.07
Kern County	Pasadena Caltech Athenaeum	52.07.21
Kern County	Taft Lincoln School Tunnel	52.07.21
San Jose	Bank of America	55.09.04
San Francisco	Golden Gate Park	57.03.22
Seattle	Olympia Highway Test Lab.	49.04.13
Taft	Taft Lincoln School Tunnel	54.01.12
Parkfield	Cholame Shandon Array 2 (*)	66.06.27
Parkfield	Cholame Shandon Array 5	66.06.27
Parkfield	Cholame Shandon Array 8	66.06.27
San Fernando	Pacoima Dam	71.02.09
San Fernando	4680 Wilshire Blvd., L. A.	71.02.09
San Fernando	120 North Robertson Blvd., L. A.	71.02.09
San Fernando	Castaic Old Ridge Route	71.02.09
San Fernando	8244 Orion Blvd., L. A.	71.02.09
San Fernando	250 E First Street, L. A.	71.02.09
Lima	La Molina	74.11.09
Olympia	Federal Office Bldg., Seattle	65.04.29
Santa Barbara	Santa Barbara Courthouse	41.06.30
SMART-1-33	33-E02	85.06.12
SMART-1-33	33-C02	85.06.12
SMART-1-39	39-E02	86.01.16
SMART-1-39	39-C02	86.01.16
SMART-1-41	41-E02	86.05.20
SMART-1-41	41-C02	86.05.20
SMART-1-43	43-E02	86.07.30
SMART-1-43	43-C02	86.07.30
SMART-1-45	45-E02	86.11.14
SMART-1-45	45-C02	86.11.14
Northridge	Pacoima Dam	94.01.17
Northridge	New Hall	94.01.17
Northridge	Arleta Fire Station	94.01.17
Northridge	Sylmar Hospital	94.01.17
Northridge	Santa Monica City Hall	94.01.17

(*) Events for which only one record was available.